Polymer 50 (2009) 4584–4595

Contents lists available at ScienceDirect

Polymer

journal homepage: www.elsevier.com/locate/polymer

Quantitative evaluation of fractionated and homogeneous nucleation of polydisperse distributions of water-dispersed maleic anhydride-grafted-polypropylene micro- and nano-sized droplets

J. Ibarretxe [a,b], G. Groeninckx [b], L. Bremer [a], V.B.F. Mathot [a,b,*]

[a] DSM Research, PO Box 18, 6160 MD Geleen, The Netherlands
[b] Katholieke Universiteit Leuven, Department of Chemistry, Division of Molecular and Nanomaterials, Celestijnenlaan 200F, Heverlee 3001, Belgium

ARTICLE INFO

Article history:
Received 30 April 2009
Received in revised form
25 June 2009
Accepted 28 June 2009
Available online 22 July 2009

Keywords:
Homogeneous nucleation
Nucleation kinetics
Polypropylene

ABSTRACT

The nucleation processes in waterborne Maleic Anhydride-grafted-Polypropylene micro- and nano-droplet suspensions have been studied. Compared to a previous report on this topic, an extended set of samples in combination with improved particle size distribution data of the samples have been used, which are both essential for the advancement of the analysis.

Self-nucleation was utilized to ensure that the observed lowered fractionated crystallization (peak) temperatures – down to the extremely low value of 34 °C – are due to a lack of seeds in the droplets, which seeds for the polypropylene system used are normally active at the heterogeneous crystallization temperature of approximately 110 °C. An unusual self-nucleation behavior was observed in case of samples having a large amount of small droplets, requiring an extremely low self-nucleation temperature in order to suppress all crystallization at the lowest temperatures. Such behavior was observed for block copolymers but has not been reported so far for droplets dispersed in an immiscible matrix, polymeric or not. Another unusual behavior was observed for some self-nucleation temperatures for which apparently two different populations of self-nuclei are created that are suggestive of the α_1 and α_2 crystal structures of isotactic polypropylene.

Next, two new methods are presented to quantify various crucial parameters of the nucleation process: one estimates the density of nucleants acting at different temperatures from the combination of dynamic DSC data and particle size distribution (PSD) data, and the other one focuses on the nature of the nucleation mechanism using both isothermal DSC data and PSD data, quantifying the nucleation rate at different temperatures. For the present MA-g-PP dispersions the latter method leads to the conclusion that the lowest crystallization temperatures reflect sporadic nucleation, probably by way of volume (homogeneous) nucleation.

In the field of polymer crystallization, polymer dispersions are usually treated as being monodisperse, even though that is rarely the case. This simplification is inadequate for the present calculations, which is why polydispersity has been taken into account in order to quantify the density of nucleants and the kinetics of nucleation. Though in the present study DSC data are used for the calculations, the methods developed can be easily adapted to other techniques like time-resolved X-ray, rheometry and dilatometry.
© 2009 Elsevier Ltd. All rights reserved.

1. Introduction

It is now-a-days generally accepted that in polymer particles, dispersed in a matrix, fractionated crystallization at increased supercooling is the consequence of the lack of high-temperature active nucleating impurities in part of the particles and the presence of lower-temperature active ones in the remaining part of the particles, and that in case of complete absence of active impurities homogeneous nucleation occurs at even higher supercoolings [1–9]. Especially relevant to the topic of this paper are the reviews published by the group of Müller on fractionated crystallization phenomena for polypropylene [10], which covers the findings on fractionated and homogeneous nucleation for isotactic polypropylene, and on the crystallization phenomena observed for block copolymers [11], while these reviews also discuss more general aspects of fractionated and homogeneous nucleation phenomena.

Isothermal crystallization of dispersed polymeric materials has been commonly performed to determine quantities like surface

* Corresponding author. Present address: SciTe B.V., Ridder Vosstraat 6, 6162 AX Geleen, The Netherlands.
E-mail address: Vincent.Mathot@SciTe.nl (V.B.F. Mathot).
URL: http://www.scite.eu

0032-3861/$ – see front matter © 2009 Elsevier Ltd. All rights reserved.
doi:10.1016/j.polymer.2009.06.067

energies of chain-folded polymer and alkane crystals, (e.g. [12,13]), and homogeneous nucleation rates, (e.g. [13,14]). Mainly for simplicity of the analysis of the results, in most of the published works the dispersions were considered to be monodisperse. However, it was pointed out already by Turnbull [15] that the particle size distribution can affect the nucleation kinetics significantly. Nevertheless, there have been only a few attempts to take into account the size distribution in the analysis of experimental data (e.g. [15–18]).

Besides, nucleation at very low temperatures has been commonly attributed to homogenous nucleation without clear proof, as has been demonstrated by Barham et al. who found that the previously reported homogeneous crystallization temperatures for polyethylene were too high [19].

In this paper the nucleation rate and nucleation density of Maleic Anhydride-grafted-Polypropylene (MA-g-PP) dispersed in water are studied in detail. First, the results of self-nucleation experiments are presented in order to ascertain that the increased supercooling is due to a lack of the most (high-temperature-) active heterogeneities in the polymer droplets. Then, particle size distribution (PSD) data are used in combination with standard cooling DSC measurements in order to estimate the number of heterogeneities active at the various temperature ranges where DSC peaks are observed in samples displaying fractionated crystallization. Moreover, isothermal DSC and particle size data are also treated with the aim of determining whether the nucleation observed at the lowest crystallization temperature is due to sporadic nucleation, and to evaluate the nucleation rate at that temperature.

The analysis proposed here is generic and can be applied to any crystallisable material dispersed in a matrix having any particle size distribution. Thus, the methods can also be applied to experimental crystallization data obtained by techniques other than DSC by applying a few simple modifications.

2. Experimental

2.1. Materials

The polymer used in this study is a Maleic Anhydride-grafted-Polypropylene (MA-g-PP), Epolene E43, produced by Eastman Kodak. The polypropylene of the MA-g-PP is a highly isotactic molecule containing 7.8 mass% maleic anhydride and having a weight average molar mass of 9000 g/mol. The surfactant used is a polyethylene oxide [15] hydrogenated talloamine, $RN(C_2H_4O)_x$-$H(C_2H_4O)_YH$, where $X+Y=15$ in average and R is an alkyl group from hydrogenated tallow. The dispersions were prepared at temperatures above the melting point of MA-g-PP and under the pressures resulting from the evaporation of water due to the increased temperatures. To this end, the materials were loaded in an autoclave, heated to the desired temperature (175 °C–200 °C), stirred for some time (20–40 min) and then cooled down to room temperature. The materials used and the method of preparation of these dispersions have been explained in more detail elsewhere [20]. The details of the preparation of the eleven dispersions to be discussed are shown in Table 1.

2.2. Methods

For the DSC measurements a Perkin Elmer Pyris-1 was used. High-purity nitrogen was utilized as purge gas. High-pressure stainless-steel pans (Perkin Elmer's product number B0182901) were chosen to ensure that the water remained liquid up to the highest measuring temperatures. Sample masses ranged from 10–15 mg (including water mass). Three kinds of DSC measurements were carried out: standard cooling measurements; self-nucleation measurements and isothermal measurements after cooling from the melt. The standard cooling measurements and the self-nucleation measurements were performed at 5 °C/min. Isothermal measurements were done after cooling at 5 °C/min from the melt and then holding the sample at the desired isothermal crystallization temperature until the crystallization was completed.

Prior to all DSC experiments the thermal history of the dispersed polymer was completely erased by keeping the sample for 5 min at 190 °C, which is 30 °C above the final melting point of the MA-g-PP used.

The self-nucleation experiments were performed following the procedure published by Fillon et al. [21]. After erasing the thermal history the sample was cooled down to 0 °C at 5 °C/min, heated up to a temperature close to the final melting point, T_s, at 5 °C/min, kept there for 5 min, cooled down to 0 °C at 5 °C/min, and finally heated up to 190 °C at 5 °C/min. Here the cooling curve after holding at T_s and the subsequent heating curve are presented.

For the PSD determination, dynamic light scattering measurements were performed using a back-scattering set-up (ALV-NIBS High Performance Particle Sizer, ALV Gmbh, Langen, Germany), operating at angle of 173° and at a wavelength $\lambda = 632.8$ nm (He/Ne laser, with output power of 3 mW). The conversion of the correlation function into the diffusion coefficient and into the particle size distribution was made automatically by the software. This method has accuracy limitations due to the assumptions made in the mathematical model used by the software to convert the measured data into size distributions. Besides, interpretation of the scattering data becomes erroneous for particles larger than 1–3 μm because the effect of gravity overrules Brownian motion, which is the phenomenon this method is based on.

In addition, the mathematical method for conversion of the correlation function into a diffusion coefficient and then into

Table 1
Formulation parameters of the MA-g-PP dispersions prepared in the pressure vessel.

Sample	I	II	III	IV	V	VI	VII	VIII	IX	X	XI
Polymer content (mass %)	24.2	25.2	27.0	29.0	29.5	18.6	22.6	23.1	23.0	25.0	41.5
Surfactant content (mass %)	1.3	1.4	0	0	1.7	3.6	1.3	1.3	1.3	3.0	11.8
KOH content (mass %)	1.0	1.1	2.6	2.8	2.7	1.8	2.1	2.1	2.1	2.4	4.0
Water content (mass %)	73.4	72.4	70.4	68.2	66.1	76.0	74.0	73.4	73.5	69.6	42.7
Emulsification temperature (°C)	185	185	200	200	190	165	185	190	185	165	200
Main stirrer speed (rpm)	300	80	300	300	300	100	80	300	300	300	350
Secondary stirrer speed (rpm)	0	0[a]	1250	1250	1000	400	0[a]	1000	1000	1000	1000
Emulsification time (min)[b]	30	35	40	40	30	30	30	30	30	15	30
Protocol type[c]	1	1	1	1	1	1	1	1	2	1	2

[a] The main stirrer was replaced by another one having a slightly different design while the secondary ones were removed.
[b] Processing time at the indicated emulsification temperature and stirring speeds.
[c] 1 stands for the protocol in which all materials were loaded from the beginning of the experiment and 2 for the protocol in which extra water was added during the emulsification.

a particle size distribution is based on algorithms derived for unimodal dispersions. Thus, if the dispersions are not unimodal an extra source of error is introduced.

As a result, the particle size distribution assessments presented in this paper, and the conclusions based on the calculations made thereof, should be interpreted bearing these limitations in mind.

An Olympus BH-2 optical microscope with a JVC TK-C1381 video camera was used for optical microscopy measurements. For the determination of the density of heterogeneous nuclei acting at the usual crystallization temperature, a sample of known thickness (200 μm) was cooled down from 200 °C to room temperature between two glass slides in a Mettler hot stage and monitored by optical microscopy. The cooling rate was 5 °C/min in order to replicate the conditions of the DSC experiments. The number of spherulites formed in a known image area – and thus, known sample volume – was then manually counted and converted into a number of spherulites per unit volume. Each spherulite is assumed to have grown from a single seed and thus the density of seeds could be estimated.

This method may introduce some error in the final result since it is highly probable that some spherulites have gone unnoticed being hidden behind bigger ones. A second source of error could be the wall-effect due to the presence of the limiting glass slides between which the polymer is contained. Indeed, nucleation could be triggered by the glass and therefore the amount of spherulites could be higher in that region or, if the glass doesn't affect nucleation, in the vicinity of the glass the density of spherulites should appear a little lower than in the bulk. Therefore, the thickness of the polymer sample was chosen to be large enough to easily host many fully developed spherulites – to diminish the influence of the glass slides – and at the same time to be thin enough not to miss too many spherulites growing behind other ones. Therefore, the error is estimated not to be larger than one order of magnitude, which is adequate for the purpose of this article.

3. Results and discussion

3.1. Particle size

Dispersions of MA-g-PP in water having particle sizes ranging from a few micrometers to submicron diameters were prepared, as previously reported [20]. A total number of eleven samples have been chosen instead of the five dispersions discussed in the previous paper in order to improve the statistics of the estimation of the number of nucleating impurities existing in the polymer, which determination will be presented hereafter. The samples chosen show the three sought nucleation behaviors, i.e. heterogeneous nucleation, fractionated crystallization, and nucleation in a single step at a maximum degree of supercooling, which possibly reflects homogeneous nucleation. The PSD data published in [20] were obtained with a Coulter LS230, which has a lower size limit of 0.04 μm. This resulted to be above the minimum particle size present in the samples. In Fig. 1 PSD data covering the whole range of sizes present in the samples and obtained by DLS are shown. Besides, Table 2 provides the number and volume percentage average particle sizes of the samples. The samples have been named and ordered according to the PSD measurement, samples S-I and S-XI being the ones with the largest and the smallest size averages, respectively. The five dispersions used in our previous paper, which are named A, B, C, D and E, are included here as well: S-I corresponds to former Sample A, S-III to Sample B, S-VI to Sample C, S-V to Sample D and S-XI to Sample E.

Samples S-IX and S-X, and S-XI, lie within the size range that can be correctly measured by DLS (see Fig. 1). Besides, for samples S-IX and S-XI the (number percent) size distributions are practically unimodal, and although the size distribution of S-X is clearly bimodal its polydispersity is very low. Thus, the characterization of the size distributions of these three samples is expected to be accurate.

On the other hand, samples S-I to S-VIII contain multimodal, broad PSDs, with particle sizes clearly extending to values above 3 μm. The correct assessment of the PSD of these samples using DLS is difficult and the results have a poor reliability. Besides, probably due to the large size of some of the particles (or maybe agglomerates), the reproducibility of the measurements was seen to be low since a single large particle crossing (or not) the laser beam during the measurement will alter the results considerably.

A sample preparation problem may also have been interfering with the DLS measurements since the dispersions were diluted prior to the evaluation of the PSD. Therefore, the data from DLS will be used taking into account that for this reason the data could be inaccurate to some extent.

In addition to the limitations for the assessment of the characteristic particle sizes, also the shape of the size distribution of the sample renders it sometimes complicated to sort these samples according to the PSD data since the number average particle size (D_n) and the weight average particle size (D_w) don't always follow the same trend. This is the case for the ordering of samples S-III and S-VI, S-IV and S-V, S-V and S-VI, and S-VII and S-VIII. In the case of the pair S-IV and S-V, the sample classified in Table 2 as having larger particles shows a lower D_w and a higher D_n. On the other hand, for the rest of the pairs it is D_n which doesn't agree with the ordering presented in the Table.

Two important concepts have to be clarified at this point. First, D_n is very influenced by small particles, while D_w is mainly determined by the large ones. Secondly, concerning the amount of polymer crystallizing at each temperature, the total mass (or volume) of the droplets of each size range is important, yet not their amount. Thus, the volume average diameter is more important than the number average diameter in this kind of study. Therefore, the chosen order is given by the evolution of D_w. This is especially of importance in case of samples S-III and S-IV, S-V and S-VI and S-VII and S-VIII.

The DSC curves shown in Fig. 2 are of great assistance to understand the adopted order for the pair S-IV and S-V. In this case it is observed that the sample having a lower D_n, i.e. S-V, provides more crystallization at low temperatures, thus in accordance with the trend in D_n, see Fig. 1a. At the same time, the same sample has a larger D_w and provides more crystallization at high temperatures, see Fig. 1b, which is what would be expected as well. Thus, compared to sample S-IV, sample S-V shows more low-temperature crystallization and at the same time also more high-temperature crystallization, while S-IV shows more intermediate crystallization. Therefore it becomes difficult to chose the right order in such a case. However, the order is not significant for the analysis performed and thus the fact that it is difficult to establish one does not pose any further contrariety.

In the pairs in which the D_n order is altered the situation is similar. Taking as an example the pair S-V and S-VI, it is observed that sample S-V having a higher D_w shows more heterogenous nucleation, as expected. It also has a lower D_n and therefore more low-temperature crystallization would be expected. Compared to S-VI the lowest crystallization temperature is slightly higher but it shows almost no intermediate crystallization. This behavior would be expected from a sample with a strong bimodality in which the large-size population lies above the size limit for which lower crystallization-temperature peaks appear and the small-size population lies below the limit for which a single crystallization peak at a maximum degree of supercooling appears. This is most likely the situation here, as suggested by the number and volume percent PSDs.

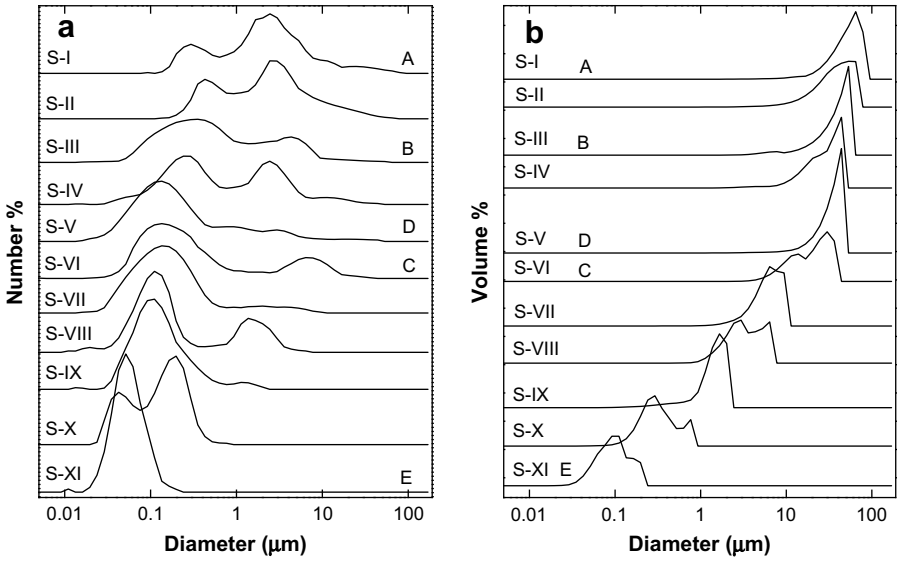

Fig. 1. (a) Number percentage and (b) volume percentage particle size distributions by DLS of samples S-I to S-XI.

3.2. Self-nucleation

Self-nucleation is a well known method in the field of crystallization of polymers in which the sample is thermally treated in order to create a number of partially unmelted crystallites that act, upon cooling, as extra nucleants [21]. This method has been used to prove that the observed extra supercooling in dispersed polymers is due to the presence of droplets free of impurities that are capable of acting at the bulk crystallization temperature, (e.g. [22,23]). In a polymer sample dispersed as particles in a matrix, the production by this method of enough seeds leads to a situation in which all polymer particles contain entities that are active as nucleants and that trigger crystallization at temperatures equal or higher than the bulk crystallization temperature. The effect of the experiment is clearly visible – even when the polymer is not dispersed – as illustrated in Fig. 3, where the self-nucleation experiment results for neat MA-g-PP are presented. The corresponding highest temperatures in the melt, chosen for the study of self-nucleation and named hereafter the "self-nucleation temperature", T_s, are plotted next to each curve.

In the case of neat MA-g-PP, for starting temperatures in the melt above (approximately) 165 °C, both subsequent crystallization and melting remain unchanged. Below 165 °C, the crystallization peak starts to shift to higher temperatures and to broaden, meaning that self-nucleation has set in. As T_s is decreased, the crystallization peak moves towards higher temperatures. This is because at lower T_s the number and size of the remaining crystallite residues is larger, and therefore crystal growth can proceed at more locations simultaneously resulting in a magnified overall crystallization rate.

Similarly, the self-nucleation effects are also visible in the melting curves for T_s below 165 °C. In Fig. 3(b) a slight change is observed in the melting curve for $T_s = 162$ °C with a little enlargement of the first melting peak. For $T_s = 160$ °C the enlargement is much more marked and at the same time a shift towards higher temperatures is observed. These two tendencies are confirmed for $T_s = 158$ °C. Indeed, crystallites formed at higher temperatures are thicker and also have a higher degree of perfection, and this leads to higher melting temperatures. Also a larger amount of polymer crystallizes as a consequence of the multiplied number of nuclei. This can be deduced from the broadening of the crystallization peaks in the DSC cooling traces of Fig. 3(a) and more clearly recognized from the enlargement of the melting peaks of Fig. 3(b), involving in both cases a larger enthalpy of transition and therefore a larger amount of polymer involved. The increase of both

Table 2
Number average (D_n) and mass average (D_w) particle size data for eleven dispersions named S-I to S-XI, as obtained by dynamic light scattering measurements.

	A		B		D	C					E
	I	II	III	IV	V	VI	VII	VIII	IX	X	XI
$\mathbf{D}_n$ (μm)	4.5	4.3	1.9	2.1	1.1	1.9	0.42	0.59	0.19	0.15	0.06
$\mathbf{D}_w$ (μm)	52.3	39.4	38.4	29.4	34.3	21.3	6.3	3.6	1.4	0.36	0.10

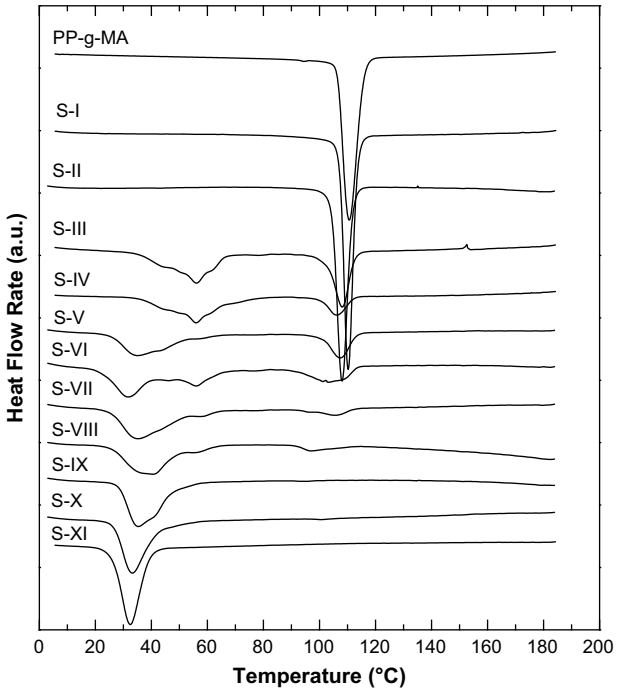

Fig. 2. DSC cooling curves of neat MA-g-PP (top) and samples I to XI.

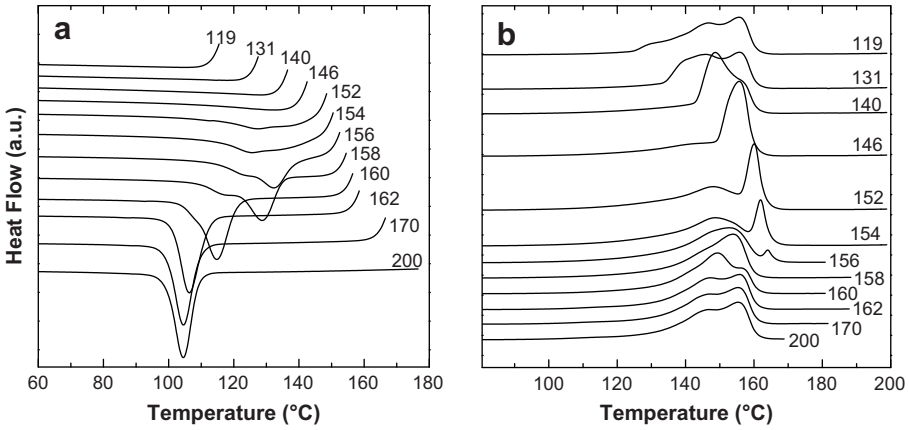

Fig. 3. DSC curves of neat MA-g-PP including curves showing self-nucleation. (a) Cooling from various temperatures in the melt and (b) subsequent heating. The highest temperatures in the melt/self-nucleation temperatures (T_s °C) are indicated next to the curves.

the melting and crystallization enthalpy is noticed in the T_s range between 165 °C and 158 °C as T_s is decreased.

If T_s is lowered to 156 °C, the broadening and shifting of the crystallization peak are still seen. Expectedly, the crystallization enthalpy seems to be lower than for higher T_s values. In addition, a new melting peak appears for this T_s. This new melting peak appears on the high-temperature side of the melting peaks, at a slightly higher temperature than the other peaks. At this point, the method applied leads besides to self-nucleation also to annealing. When a low enough self-nucleation temperature is used, the part of the polymer that remains unmelted becomes large. The unmelted crystallites were kept at T_s for a few minutes and at this temperature they undergo annealing and by that reorganization into more perfect and/or larger structures. When the polymer is cooled down in the next step, a smaller amount of material can crystallize since part of it was never melted. Then, during the subsequent heating, two melting events can be observed: one at lower temperatures for the crystallites that have formed during the cooling step, and a second one at higher temperatures for the crystallites that were annealed at T_s. Since the perfection/size of the annealed crystallites is higher/larger respectively, they melt at higher temperatures.

If T_s is decreased further, more material remains unmelted during the self-nucleation step, and therefore less crystallization is observed upon cooling leading to a larger melting peak caused by an increasing amount of annealed material. Besides, since the temperature at which the unmelted crystallites are annealed (T_s) is lower, their perfection becomes lower as well, resulting in a lower melting temperature. Thus, once annealing sets in, if T_s is lowered less crystallization is observed upon cooling, a larger part of the enthalpy of melting is due to the annealed crystallites, and these crystallites melt at increasingly lower temperatures. For very low T_s values, like 146 °C or lower, there is no visible crystallization upon cooling, except for maybe some directly after cooling starts, which is then masked by the transient starting signal of the DSC. When T_s is below 140 °C, the melting curves begin to recover the shape of non self-nucleated samples except for an extra shoulder on the low-temperature side, where annealing at low temperatures leads to perfection/size increase of the least stable crystallites. No appreciable crystallization takes place upon cooling since practically no material is melted at T_s.

Fig. 4 presents (a) the cooling curves of sample S-IV after fully erasing the thermal history and after introducing a self-nucleation step and (b) the subsequent heating curves into the melt.

As an exception to the very reproducible thermal behavior in all other dispersions, sample S-IV shows a slightly different cooling DSC curve after the first cooling and the second heating cycle. After $T_s = 168$ °C and $T_s = 164$ °C a shift towards slightly higher temperatures is observed at the high-temperature side (around 60 °C) of the low-temperature crystallization peaks.

In the cooling curves the effects of self-nucleation are first observed by lowering T_s to 164 °C causing the high-temperature

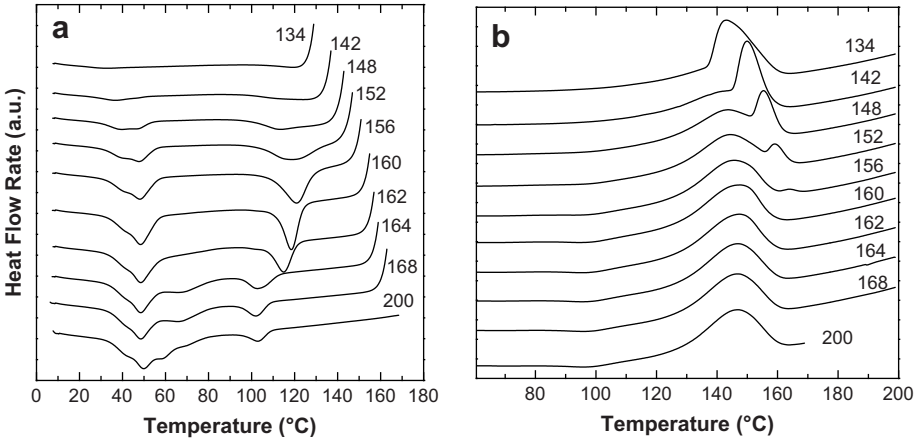

Fig. 4. DSC curves of sample S-IV, including curves showing self-nucleation. (a) Cooling from various temperatures in the melt and (b) subsequent heating. The highest temperatures in the melt/self-nucleation temperatures (T_s °C) are indicated next to the curves.

peak to be slightly larger and broader at the high-temperature side. For $T_s = 162\,^{\circ}C$, the effect is more pronounced and the high-temperature peak clearly moves to higher temperatures. Besides, the high-temperature side of the broad crystallization exotherm at lower temperatures has disappeared. Moreover, the crystallization enthalpy related to the high-temperature peak is clearly enlarged. Thus, some of the particles have been self-nucleated and they crystallize at higher temperatures than usually and to a larger extent. The bigger the particles, the higher is the crystallization temperature [20] and, for the same reason, the higher the probability of being self-nucleated. Therefore, self-nucleation affects the high-temperature ("large size") side of the DSC curve first.

As T_s is lowered towards 156 °C, the outcome follows the same trend: all low-temperature crystallization tends to disappear and adds to the peak at high temperature, which displaces towards even higher temperatures. Down to this temperature all the melting curves look unchanged regardless T_s, except maybe for a decrease in the total area of the exothermic peak around 95 °C, which corresponds to the polymer crystallizing at low temperatures. Crystallites formed at low temperatures reorganize into more perfect structures upon heating, which is observed as a broad, and seemingly small exothermic peak in the DSC curve. If, due to the self-nucleation treatment, less material crystallizes at low temperatures, then also less material will recrystallize upon heating.

The word "seemingly" is used because of the fact that the low-crystallization peak is not clearly accompanied by a melting peak at low temperatures. Most probably this is caused by strong reorganization processes (including a continuous process of (re)melting/recrystallization) during heating across a wide temperature range, and the "seemingly small exothermic peak around 95 °C " just reflects some cold crystallization/recrystallization as part of the reorganization process. Thus the melting related to the low-temperature crystallization peak shifts towards high temperatures and even merges with the high-temperature melting peak. Only by using extremely high heating rates of the order of 10 000 °C/s – dependent on the polymer at hand – the reorganization process can be effectively hindered or even suppressed by which 'real', initial melting occurs at the expected lower temperatures [24].

For $T_s = 156\,^{\circ}C$, a new melting peak appears on the right side of the usual one. This endotherm is due to the melting of crystals having a higher degree of perfection and/or have larger size resulting from annealing during the self-nucleation step. By decreasing T_s further, the low-temperature crystallization peaks become less visible but there is less crystallization at high temperature as well. At this stage, an increasingly important part of the material remains unmelted during the self-nucleation cycle and therefore less and less crystallization is observed. Finally, for $T_s = 134\,^{\circ}C$, there is almost no crystallization at low temperatures.

When the annealing is performed at lower temperatures, the crystallites addressed have lower melting temperatures, leading to a shift to lower temperatures of the resulting 'valley/peak' (meaning decreased endo/increased endo heat flow rates respectively) shaped part of the melting curve connected to the annealing temperature, T_s. In addition, it is noticeable that shifting annealing to lower temperatures increases the amount of material involved, which is reflected by an increase in enthalpy of fusion of the part of the melting curve addressed. That is very apparent if one compares the melting curves after self-nucleation at 152 °C and at 142 °C.

For low T_s values (134 °C and below), most of the material remains unmolten. Hence, what is observed in the heating curve is a superposition of the usual melting curve with the valley/peak due to the annealing of crystallites.

In the extreme case of sample S-XI, having an unimodal PSD situated in the sub-μm region, the DSC cooling curve from 200 °C downwards only exhibits a low-temperature crystallization peak. Interestingly, Fig. 5 shows that upon cooling after $T_s = 160\,^{\circ}C$, a small crystallization peak of unknown origin is evident around 135 °C. This phenomenon seems to move to slightly higher temperatures when T_s is decreased to 158 °C by which crystallization starts immediately upon cooling.

For sample S-XI, self-nucleation of the low-temperature crystallization peak starts at the same $T_s = 152\,^{\circ}C$ as in case of sample S-IV. Unexpectedly, for this self-nucleation temperature, a new, broad crystallization exotherm appears around $T_s = 113\,^{\circ}C$ in addition to a crystallization event taking place during the start of the cooling. Speculatively, there are two populations of self-nuclei with different activities. In the case of MA-g-PP this original behavior could be explained considering the α_1 into α_2 transition sometimes taking place upon heating [25,26] and which has been observed to happen at approximately 150 °C in the polymer discussed here [20]. If T_s is such that self-nuclei of both the α_1 and α_2 modifications of the monoclinic polymorph of MA-g-PP are present, upon cooling the most perfect nuclei (α_2) could trigger crystallization at higher temperatures (around 135 °C) and the less perfect nuclei (α_1) would only activate once lower temperatures (around 113 °C) are attained. This phenomenon can only happen for T_s values in the range where α_1 and α_2 coexist, which is probably the case in these measurements.

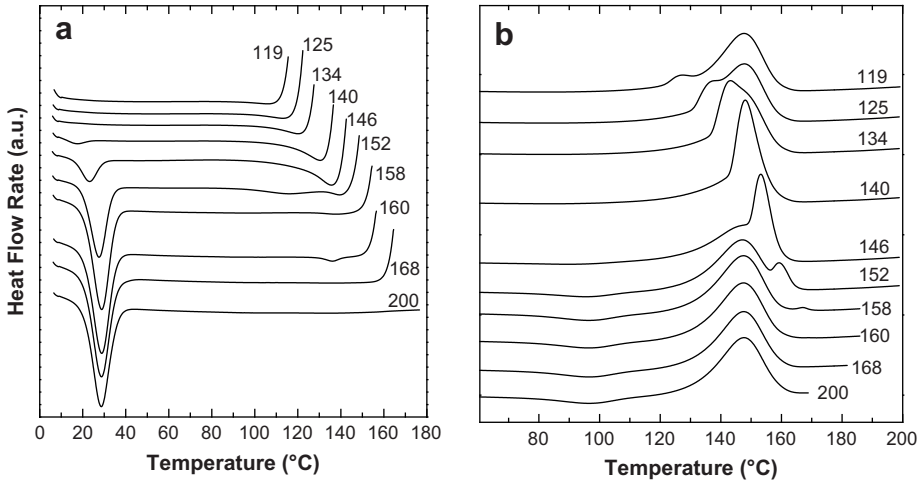

Fig. 5. DSC curves of sample S-XI, including curves showing self-nucleation. (a) Cooling from various temperatures in the melt and (b) subsequent heating. The highest temperatures in the melt/self-nucleation temperatures (T_s °C) are indicated next to the curves.

For sample S-XI it is necessary to decrease T_s to 134 °C to eliminate all crystallization at low temperatures, while still observing some crystallization at the start of the cooling. The melting curves are very similar to those of sample S-IV. Signs of annealing appear approximately for the same T_s and they become more important as T_s is lowered. There is one additional observation to be done in the melting curves of both samples, although it is more evident for S-XI. During heating the DSC traces display a broad exotherm around 95 °C due to the reorganization of the low perfection/small crystallites, formed at low temperatures, into more stable ones. For the curves where the self-nucleation technique is efficient, the reorganization process is less important or even vanishes completely due to the decrease of the amount of material crystallizing at low temperatures.

According to Fillon et al. [21], usually three domains exist in which T_s may be situated. In the case of S-IV domain II (self-nucleation domain) extends from 164 °C to 156 °C for the largest particles. However, for the smallest particles, domain II is not existent and in order to self-nucleate them domain III (self-nucleation and annealing domain) has to be reached. Sample S-XI behaves similarly, and in this case most of the particles require very low T_s in order to undergo self-nucleation. Absence of domain II in block copolymers has previously been reported [11,27], but it has never been observed for dispersions of crystallisable polymers in an immiscible matrix. This anomalous behavior is due to the vast number of self-nuclei necessary to switch the low-crystallization temperature of a large number of droplets to higher temperatures, which requires a very low T_s.

3.3. Estimation of the density of nucleants

By counting the number of spherulites resulting from crystallization during cooling from the melt at 5 °C/min of a sample of neat MA-g-PP of known volume, it was possible to estimate the amount of nucleation sites per unit volume from optical microscopy measurements. The resulting value was approximately $\sim 10^6$ nuclei/cm^3. The calculation was performed as explained in the experimental section. The observed nucleation process was thermal, with new nuclei forming continuously during cooling until crystallization ended.

Even in the case of an even distribution of nucleants across the polymer droplets, 10^6 nuclei/cm^3 would just be approximately enough to heterogeneously nucleate the totality of the droplets present in a sample having just one droplet size of 100 μm-diameter. The sizes of the droplets in all samples presented here are smaller than that and thus it would be expected that in the samples, at most, only partial heterogeneous nucleation at the highest temperature could occur. Notwithstanding this outcome of the reasonable calculation, the DSC cooling curves clearly reveal that for two of the dispersions nucleation takes place exclusively heterogeneously and at nearly the same temperature as in the bulk, i.e. triggered by the same type of nucleants. Therefore, it is obvious that the nucleation density estimated from the bulk is not fully representative of the situation in the dispersions. An explanation of this difference is that in the bulk many of the seeds will not have the opportunity to trigger primary nucleation because the most active ones have already formed enough crystallites to space-fill the whole sample volume. In the dispersions each droplet acts independent of the rest and they all need to be nucleated separately. Since the size of the droplets is smaller than the average spherulite size formed in the bulk, a larger number of impurities have the chance to become active, which however, in turn, requires a slightly higher degree of supercooling than in the bulk resulting in the slightly lower crystallization temperatures of samples S-I and S-II, see Fig. 2.

In order to estimate more precisely the number of nuclei acting at the highest crystallization temperature observed for MA-g-PP, the combination of PSD data and DSC crystallization curves has been analyzed in detail.

When considering the results of this analysis, it should be born in mind that the nucleation density could be affected by the processing of the samples [28], or by the composition if any of the components stimulates or hinders nucleation [29]. Moreover, the confinement of MA-g-PP by small domains could also affect the nucleation density. For the data treatment presented further on it is assumed that the heterogeneous nucleation density doesn't vary with composition and particle size or during the processing. It is also assumed that the polymer droplets that undergo nucleation are completely consumed and cannot experience further nucleation at lower temperatures. This assumption is justified by the behavior observed in the bulk and in samples S-I and S-II where, once crystallization has happened, there is no further nucleation at lower temperatures. In the dispersions, the developed crystallinity is affected by the particle size and crystallization temperature [20]. The temperature dependence of the crystallization enthalpy is known [30] and has been taken into account for the calculations [31]. A confinement dependence of the crystallinity has been observed in the samples as concluded from crystallinity data published previously [20]. The data presented in that paper show that the crystallinities of neat MA-g-PP and of sample S-I are slightly different, being lower in the dispersion, even though crystallization occurs at practically the same temperature in both of them. This effect is difficult to account for and it might be an error source in the determination of the amount of particles, especially for the lower crystallization-temperature peaks, shown by smaller particles.

It has been shown that a non-monodisperse character of the dispersions affects nucleation in a significant manner [16–18] and therefore the PSD data were used for the analysis, instead of the average diameter values. To this end, the discrete size classes provided by the ALV-NIBS High Performance Particle Sizer were used, treating each of these size classes as strictly monodisperse.

The probability of occurrence of seeds in the MA-g-PP follows a Poisson distribution [32]. Thus, the probability for a particle of volume V of a MA-g-PP containing N nuclei/cm^3 to contain one or more impurities (i.e. to undergo heterogeneous nucleation) is given by:

$$P = 1 - e^{-N \cdot V} \tag{1}$$

The enthalpy of crystallization per size class produced by nucleation by a certain type of impurity can be calculated as

$$\Delta H_i = V_i \cdot \Delta h_c \cdot P_i \tag{2}$$

where V_i is the total volume of the droplets in class i, Δh_c is the enthalpy of crystallization per unit volume, and P_i is the probability of crystallization of the droplets in class i. The summation to all classes i of Equation (2) in combination with Equation (1) leads to the total enthalpy of crystallization at the considered temperature:

$$\Delta H = \sum_i V_i \cdot \Delta h_c \cdot \left(1 - e^{-N \cdot V_i}\right) \tag{3}$$

Since the enthalpy of crystallization induced by each type of nucleating impurity can be calculated from DSC experimental data, the only unknown in Equation (3) is the density of nuclei N, which therefore can be calculated. Then, using the density of nuclei formed at the considered crystallization temperature the PSD of uncrystallized droplets can be calculated. The method can then be applied to other crystallization temperatures, obtaining the number of nuclei acting at each crystallization temperature in

a sample where fractionated crystallization is observed. Finally, the total density of active impurities can be calculated by adding the density of nuclei obtained for each crystallization temperature.

The accuracy of these estimations is mainly determined by the accuracy of the PSD assessment, the degree to which different crystallization temperatures (types of nuclei) can be properly differentiated in the DSC curves, and of course by the correctness of the assumptions stated before. Table 3 reveals the results of the estimation of the number of impurities for two crystallization temperatures (110 °C and 54 °C). These temperatures have been chosen as being the ones present in the largest number of samples. Many more DSC peaks are observed in the curves of Fig. 2 but, although theoretically possible, in practice the available PSD data lack the accuracy needed to consider them all separately. Besides, most of the intermediate peaks are not isolated but overlapping each other and the way to deconvolute the enthalpies for each type of impurity is arbitrary. For this reason, for the crystallization at 54 °C broad crystallization regions were taken as resulting from a single crystallization phenomenon. The third data column of the Table displays the maximum amount of active impurities that can be present in the MA-g-PP if samples S-IX, S-X and S-XI are to crystallize solely at the lowest crystallization temperature, as seen from the DSC cooling traces of Fig. 2. These values were estimated using Equation (3) to find the maximum N value for each of the three samples for which crystallization – triggered by that density of impurities – would account for less than 1% of the total crystallization. That 1% limit was chosen as a value below which the heterogeneous crystallization would be difficult to observe by DSC. The so estimated N is not at all the actual density of nuclei of the three samples, but the upper limit for that density.

It is clear from Table 3 that the figures obtained for each dispersion vary notably, covering a range of nearly three orders of magnitude for the case of crystallization at 110 °C, and even more for crystallization at 54 °C. First of all, the determination of the enthalpy of crystallization at each temperature and its transformation into crystallized mass of MA-g-PP is not unambiguous. The presence of overlapping DSC peaks renders the task difficult. Moreover, the lack of accuracy of the PSD determination accounts for an important part of the discrepancies, as pointed out before. Nevertheless, the averages of the number of impurities seem to be consistent with the maximum number of active impurities obtained for samples S-IX, S-X and S-XI and presented in the third data column of Table 3. It is possible to observe in Fig. 2 that sample S-XI undergoes crystallization in a narrow temperature range resulting in a narrow DSC peak. The DSC peak of S-IX is narrow as well, but a small shoulder is visible on the high-temperature side. This shoulder, although ignored for the calculation of the amount of impurities, indicates that in a tiny fraction of the droplets of the sample nucleation is triggered at slightly higher temperatures. The cause for this shoulder could be the existence of a small fraction of particles having relatively large sizes that crystallize in absence of seeds [18] but it could also be that the amount of nuclei is just large enough to trigger a little but distinguishable heterogeneous nucleation. The PSD data show that the average particle size is more than one order of magnitude larger in sample S-IX than in S-XI, which explains the presence of the higher temperature crystallization, but it is not enough to discern the nature of the shoulder.

Table 3
Estimation of the number of impurities active at two different temperatures (110 °C and 54 °C) and the maximum possible amount of impurities per gram of MA-g-PP for samples S-IX, S-X and S-XI assuming full crystallization at the lowest temperature.

	110 °C	54 °C	Max. Amount
S-I	1.5E + 09	–	–
S-II	5.0E + 09	–	–
S-III	1.8E + 07	1.5E + 10	–
S-IV	8.2E + 06	2.0E + 10	–
S-V	1.3E + 07	4.0E + 06	–
S-VI	3.9E + 07	1.1E + 08	–
S-VII	4.0E + 08	5.6E + 08	–
S-VIII	2.5E + 09	4.5E + 09	–
S-IX	–	–	1.0E + 09
S-X	–	–	1.0E + 11
S-XI	–	–	1.0E + 13
Geom. Average	1.7E + 08	8.3E + 08	–

For the analysis presented above it was assumed that only the lowest crystallization temperature is due to impurity-free nucleation, but so far there is no proof to state that crystallization at other temperatures is triggered by impurities. Reports exist on homogeneous nucleation of Polyethylene oxide happening at different temperatures due to considerable differences in particle size [18]. In principle this could be the reason for observing so many crystallization peaks at lower temperatures and especially the reason for having the lowest crystallization temperature ever reported for iPP in this kind of experiments [20,33]. Nevertheless, according to the reasoning of Massa et al. [18], a sample with a broad but continuous PSD cannot show a discrete crystallization behavior. Thus, since in some of the samples discussed here nucleation occurs both at the lowest temperature as well as at higher temperatures – while the nucleation events occur at discrete temperatures and not across a very broad range of temperatures extending down to the lowest temperature – the possibility that several of the observed crystallization peaks are due to homogeneous nucleation can be ruled out.

It is therefore reasonable to assume that intermediate crystallization peaks are due to heterogeneous nucleation, and therefore not intrinsically different from the origin of the highest temperature crystallization peak. As for the lowest temperature peak, in the next section a deeper insight into its nature will be given.

3.4. Nucleation kinetics

If we assume that once a droplet is nucleated the crystallite formed covers the entire droplet volume fast enough, then only one primary nucleation event occurs in each droplet. This assumption, which is often used in the field of polymer crystallization in dispersed systems, becomes increasingly appropriate as the particle size is decreased and as the supercooling is increased. In sample S-XI the particles are extremely small and crystallization takes place at extremely large supercoolings. In such a sample, the primary nucleation happening in a droplet without active impurities is random and independent [13], which is often referred to as sporadic nucleation. In a perfectly monodisperse system and at constant temperature this kind of primary nucleation is described by

$$N/N_0 = e^{-k\cdot t} \quad (4)$$

where N/N_0 is the fraction of droplets unfrozen at time t and N_0 is the total number of droplets that undergo nucleation. The definition of k depends upon whether volume nucleation, $k = I_V \cdot V$, or surface nucleation, $k = I_A \cdot A$, occurs. I_V and I_A are the volume dependent and surface dependent nucleation rates, respectively; V is the volume of the dispersed particles and A their surface area. Thus, plotting $Ln(N/N_0)$ versus t straight lines of slope – k should be obtained for sporadically nucleated samples. Fig. 6 presents the DSC isothermal crystallization data for sample S-XI.

Although not far from it, the experimental data plotted in Fig. 6 do not follow completely straight lines. This doesn't forcedly mean that the observed nucleation is not sporadic. A plausible explanation is found, once more, in the polydispersity of the PSD. Sample

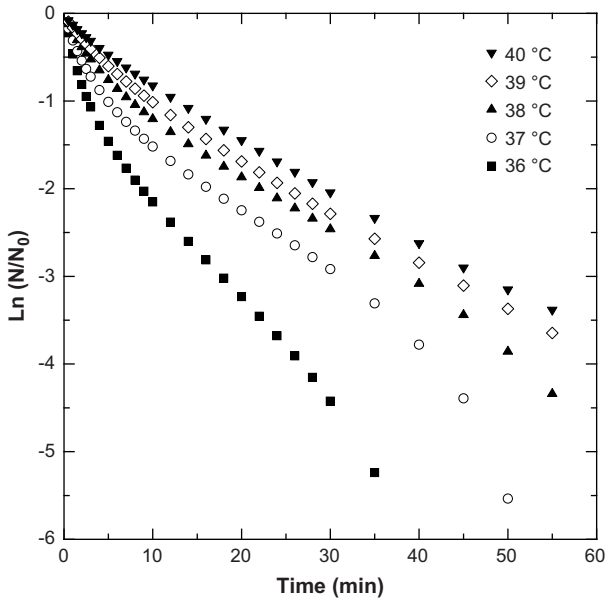

Fig. 6. $Ln[N(t)/N_0]$ based on Isothermal crystallization data of the MA-g-PP droplets in sample S-XI as a function of time and temperature.

S-XI, although the least polydisperse of all reported samples, covers a range of particle sizes of one order of magnitude. A difference in diameter of one order of magnitude transforms into a difference of two or three orders of magnitude in the exponential factor of Equation (4). The probability of developing a nucleus is proportional to the volume (or surface area) of the droplet. Larger droplets have a higher probability of being (semi-)crystalline after a certain time than smaller ones. In terms of the plot of Fig. 6 this means that particles that are larger than the average will crystallize faster and the absolute value of LnN/N_0 will be lower at shorter times than expected for a monodisperse sample when these particles undergo crystallization. But, once most of the large particles are (semi-)crystalline only the ones smaller than the average particle size remain molten and these tend to take longer time to undergo nucleation than expected for the average particle size. As a consequence, at longer times the absolute value of LnN/N_0 will be higher than for the average particle size. Thus, the plots of Fig. 6 may perfectly correspond to sporadic nucleation.

If a polydisperse polymer dispersion is considered Equation (4) is not correct [16,17]. However, if the particle size data of the dispersion are known, each size class of a discrete PSD data set can be treated as an independent, practically monodisperse system and Equation (4) can be applied for each class as follows:

$$N_i(t)/N_{0i} = e^{-k_i \cdot t} \tag{5}$$

where $N_i(t)/N_{0i}$ is the fraction of droplets of size class i unfrozen at time t and N_{0i} is the total number of droplets of class i that undergo nucleation. The definition of k_i depends upon whether volume nucleation, $k_i = I_V \cdot V_i$, or surface nucleation, $k_i = I_A \cdot A_i$, occurs. V_i is the volume of the particles of class i and A_i their surface area. The fraction of unfrozen droplets is related to the enthalpy of crystallization by

$$N_i(t)/N_{0i} = 1 - \frac{\Delta H_i(t)}{\Delta H_{Ti}} \tag{6}$$

where $\Delta H_i(t)$ is the enthalpy of crystallization of the droplets of class i at time t and ΔH_{Ti} is the total enthalpy of crystallization of the droplets of class i at the experimental temperature. The overall fraction of crystallization is calculated by considering all size classes present in the sample:

$$\Delta H(t)/\Delta H_T = \frac{\sum_i \Delta H_i(t)}{\sum_i \Delta H_{Ti}} \tag{7}$$

where ΔH_T can be calculated as

$$\Delta H_T = V_T \cdot \Delta h_T \tag{8}$$

where V_T is the total dispersed phase volume and Δh_T is the total crystallization enthalpy per unit volume. If the enthalpy of crystallization per unit volume is not influenced by the particle size, then the enthalpy of crystallization is evenly distributed over the volume of dispersed polymer and thus

$$\Delta H_i(t) = V_T i \cdot \Delta h_T \tag{9}$$

where $V_T i$ is the total volume of the droplets in size class i.

Combination of Equations (5–9) results in

$$1 - \Delta H(t)/\Delta H_T = \frac{\sum_i V_T i \cdot \left(1 - e^{-k_i \cdot t}\right)}{V_T} \tag{10}$$

In Equation (10) k_i has to be replaced by $I_V \cdot V_i$ or $I_A \cdot A_i$ for volume or surface nucleation, respectively. Then the only unknown is I_V or I_A, since V_T is one of the experimental parameters, $\Delta H(t)$ and ΔH_T are obtained experimentally from the DSC curves and V_i (or A_i) are known from the PSD data.

In practice, however, ΔH_T can be difficult to obtain experimentally using DSC. First of all, achieving the end of the isothermal crystallization may take a long time at the highest temperatures and problems of sensitivity of the DSC can be encountered at some point. Secondly, for the lowest temperatures crystallization may have started before the isothermal crystallization temperature is reached. Moreover, it has been assumed that the crystallization enthalpy is not affected by the particle size (within the size range of each sample) but the sample on which this method is applied here (i.e. S-XI) contains droplets as small as 10–20 nm, where the confinement and reduced volume may be enough to influence the

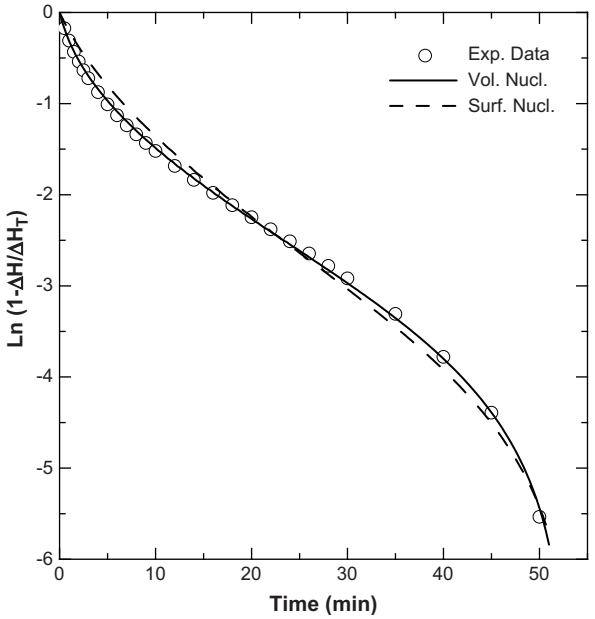

Fig. 7. Fitting of experimental isothermal crystallization data at 37 °C of sample S-XI according to volume nucleation (solid line) and surface nucleation (dashed line).

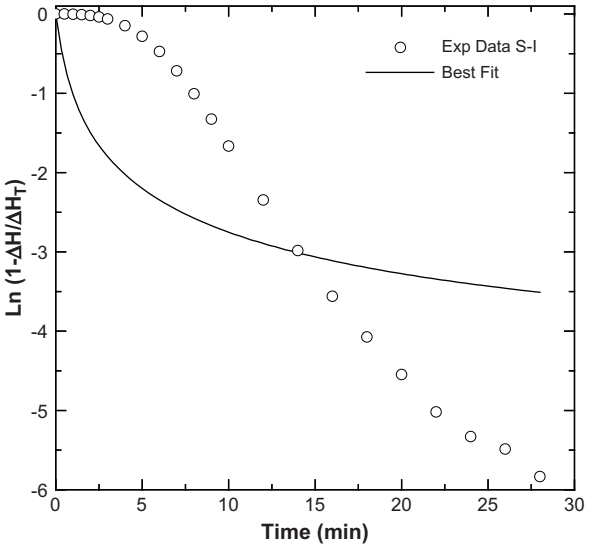

Fig. 8. (Mis)fit of experimental isothermal crystallization data at 120 °C of sample S-I according to sporadic by volume nucleation.

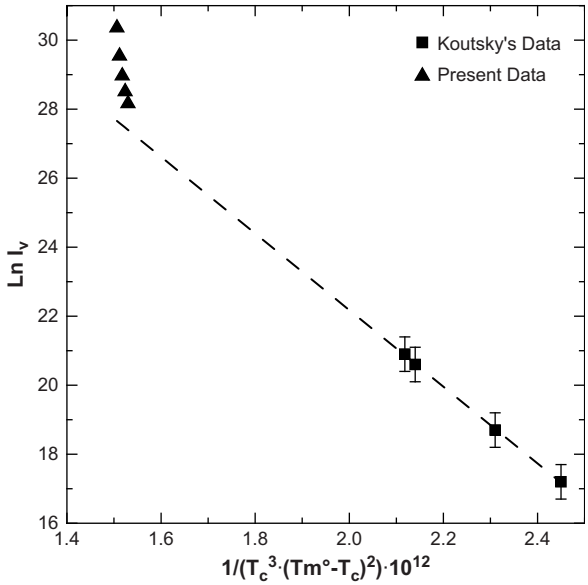

Fig. 9. Sporadic by volume nucleation rate (I_v) versus supercooling. Data obtained from isotactic PP dispersed in silicon oil (■) [14] and sample S-XI (▲). T_m° is the equilibrium melting temperature of polypropylene and is taken to be 459 K, while T_c is the isothermal crystallization temperature in K.

degree of crystallinity and/or the microstructure of the crystallites (and therefore the enthalpy of crystallization).

Therefore, in this analysis both I_V (or I_A) and ΔH_T are used as fitting parameters. A priori, it is not possible to know whether sporadic nucleation occurs and whether it is volume or surface nucleation. The fitting of the experimental data using both I_V and I_A is expected to allow discrimination between all three possibilities. In Fig. 7 the calculation based on volume nucleation fits the experimental data properly whereas the best fit for surface nucleation is less optimal. The observed crystallization clearly displays the kinetics of sporadic nucleation but, although the volume nucleation possibility seems more likely, it would be too chancy to discard surface nucleation based on the fits of the experimental data in Fig. 7.

In order to verify that it is not possible to fit the data of samples undergoing heterogeneous nucleation properly using the sporadic nucleation concept, the same treatment was applied to a system in which heterogeneous nucleation is known to occur, i.e. S-I. Indeed, fitting the experimental data in a satisfactory manner turned out to be impossible, as it is shown in Fig. 8, which presents the best fit of the isothermal crystallization data of sample S-I considering sporadic by volume nucleation. The attempt to fit the data considering sporadic by surface nucleation was also unsuccessful. In conclusion, the analysis applied is capable of discerning between heterogeneous and sporadic nucleation by either volume or surface nucleation.

Table 4 presents the nucleation rate values obtained by fitting the DSC isothermal crystallization data of sample S-XI at different temperatures considering sporadic by volume and surface nucleation, and taking into account the distribution of particle sizes.

Table 4
Sporadic by volume and surface nucleation rates obtained from fitting the DSC isothermal crystallization data of sample S-XI taking into account the polydispersity of the sample.

T_{iso} (°C)	I_v (No.Nucl./s cm^3)	I_a (No.Nucl./s cm^2)
36	1.5E + 13	2.2E + 07
37	6.8E + 12	1.3E + 07
38	3.8E + 12	8.9E + 06
39	2.4E + 12	7.9E + 06
40	1.7E + 12	6.1E + 06

Finally, the sporadic by volume nucleation data for S-XI are compared with those provided by Koutsky et al. for isotactic Polypropylene [14]. Fig. 9 shows the estimated sporadic by volume nucleation rate (I_V) versus supercooling for both sets of data.

The linear extrapolation to larger supercoolings of the data published by Koutsky et al. is not in disagreement with the values obtained here for MA-g-PP, taking into account that Koutsky et al. published data of crystallization between 84 °C and 96 °C, whereas the data presented here have been obtained at temperatures between 36 °C and 40 °C. Thus, even if we accept that in both cases the nucleation was homogenous, the temperature difference is very large and the assumptions made by the group of Koutsky (that some of the parameters used to estimate the nucleation rate remain constant over a certain temperature range) need not to hold over such a wide range [31]. Therefore, extrapolation of the values obtained by Koutsky to the temperatures dealt with in the present study need not to be linear.

4. Conclusions

The nucleation of MA-g-PP dispersed as droplets in water has been studied in detail. A set of eleven dispersions was used showing a gradual transition from fully heterogeneous crystallization around approximately 110 °C – slightly lower than the bulk crystallization of neat MA-g-PP – via fractionated crystallization to (homogeneous?) crystallization at an extremely high degree of supercooling, at temperatures around approximately 34 °C. Similar study systems were also used by Weber et al. They realized a very high supercooling by way of low-temperature polymerization of polyethylene in water leading to stable dispersions of polyethylene nanoparticles in water [34]. Also, recently Jin et al. studied the thermal behavior of confined polypropylene samples and found a supercooling comparable to the figure presented here using a different sample preparation technique that consisted in producing polypropylene nanolayers by layer-multiplying coextrusion and then obtaining nanoparticles by thermally breaking up the nanolayers [33].

The crystallization behavior of our eleven samples was studied by dynamic and isothermal DSC experiments and the data obtained were interpreted to clarify the nature of the nucleation phenomena involved.

Self-nucleation was studied by varying the highest temperature in the melt: the "self-nucleation temperature", T_s. An anomalous self-nucleation was encountered for the smallest MA-g-PP droplets in water. For these droplets, self-nucleation/domain II is completely absent and the combination of annealing and self-nucleation/domain III has to be applied to force a shift of the crystallization peaks towards higher temperatures as for neat MA-g-PP. This phenomenon has only been observed hitherto for very small domains in block copolymers. The experiments proved that the extreme extra supercooling/extremely low temperatures realized for some dispersions is only due to the lack of active impurities inside the droplets.

Interestingly, it was observed that for a certain T_s range coexistence of two types of self-nuclei is possible for MA-g-PP. These two types of seeds speculatively could correspond to the α_1 and α_2 modifications. They induce crystallization at different temperatures upon cooling, according to the perfection of the nuclei themselves, which trigger growth of crystallites of different stability. The existence of the two alpha (monoclinic) modifications is known since long, but their possible influence on the self-nucleation of MA-g-PP has gone unnoticed until now, as far as the authors know.

A method for the estimation of the number of active impurities at each crystallization step in polydisperse samples is presented as well. This procedure takes into account the influence of the particle volume in these calculations, which is seldom done in the field of polymers but which has a paramount effect on the results. Application of this method to each of the eleven samples led to nucleation densities covering three orders of magnitude approximately. Probably, the relative lack of accuracy of the PSD data, the simplistic separation of all heterogeneous crystallization into two peaks and the sometimes ambiguous determination of the enthalpy of crystallization are the causes for the discrepancies found. However, the averages of the nucleation densities estimated for each sample are consistent with the calculated maximum number of nuclei in order to still observe seed-free nucleation in sample S-IX, which sample has the largest particles among the samples that crystallize exclusively at the lowest crystallization temperature, around approximately 34 °C.

A second method for the calculation of the seed-free nucleation rate of polydisperse systems crystallizing isothermally is presented. Again, the novelty of this procedure is that it takes into account the variation in particle size. The method allows determining whether the observed nucleation is sporadic and, if so, the surface or volume nucleation rate can be calculated. Application of this method to a sample crystallizing at maximum attained supercooling proved that sporadic nucleation occurred, and most likely by volume nucleation (homogeneous nucleation).

The two procedures for treating dynamic and isothermal crystallization data are generic, and can be applied to any sample of which the PSD is well determined. Moreover, with a few simple modifications, these methods could be used to retrieve the same kind of information from other measuring techniques like time-resolved X-ray, ultrasonic spectroscopy, rheometry, etc.: bulk techniques by which crystallization can be followed as function of time. Such kind of information, together with the PSD, provides enough input for the two procedures presented here.

Acknowledgements

J.I.U. would like to thank the European Community for a Marie Curie Industry Host Fellowship grant, Contract Nr HPMI-CT-1999-00058, as well as DSM Research, the Katholieke Universiteit Leuven and SciTe B.V. for scientific and financial support. The authors also wish to thank Professor Johan Martens from the Centrum voor Oppervlaktechemie & Katalyse of the Katholieke Universiteit Leuven for the help with the dynamic light scattering measurements. Support for SciTe from the FP7 CSA project "NaPolyNet", see www.napolynet.eu, is recognized.

References

[1] Frensch H, Harnschfeger P, Jungnickel BJ. Fractionated crystallization in incompatible polymer blends, Multiphase polymers: blends American Chemical Society, and ionomers, 1989. p. 101–25 [chapter 5].
[2] Arnal ML, Matos ME, Morales RA, Santana OO, Müller AJ. Evaluation of the fractionated crystallization of dispersed polyolefins in a polystyrene matrix. Macromol Chem Phys 1998;199(10):2275–88.
[3] Groeninckx G, Vanneste M, Everaert V. Polymer blends handbook. In: Utracki LA, editor. Crystallization, morphological structure, and melting of polymer blends. Kluwer Academic Publisher; 2003. p. 203–94 [chapter 3].
[4] He Y, Zhu B, Kai W, Inoue Y. Nanoscale-confined and fractional crystallization of poly(ethylene oxide) in the interlamellar region of poly(butylene succinate). Macromolecules 2004;37(9):3337–45.
[5] Tol RT, Mathot VBF, Groeninckx G. Confined crystallization phenomena in immiscible polymer blends with dispersed micro – and nanometer sized PA6 droplets, part 1: uncompatibilized PS/PA6, (PPE/PS)/PA6 and PPE/PA6 blends. Polymer 2005;46:369–82.
[6] Tol RT, Mathot VBF, Groeninckx G. Confined crystallization phenomena in immiscible polymer blends with dispersed micro- and nanometer sized PA6 droplets, part2: reactively compatibilized PS/PA6 and (PPE/PS)/PA6 blends. Polymer 2005;46:383–96.
[7] Tol RT, Mathot VBF, Groeninckx G. Confined crystallization phenomena in immiscible polymer blends with dispersed micro- and nanometer sized PA6 droplets, part 3: crystallization kinetics and crystallinity of micro- and nanometer sized PA6 droplets crystallizing at high supercoolings. Polymer 2005;46:2955–65.
[8] Tol RT, Mathot VBF, Groeninckx G. Confined crystallization phenomena in immiscible polymer blends with dispersed micro-and nanometer sized PA6 droplets part 4: polymorphous structure and (meta)-stability of PA6 crystals formed in different temperature regions. Polymer 2005;46:2966–77.
[9] Tol RT, Mathot VBF, Reynaers H, Groeninckx G. Ch. Relationship between phase morphology and crystallization behavior in crystallizable polymer blends: fractionated crystallization and homogeneous nucleation. In: Harrats C, Thomas S, Groeninckx G, editors. Micro- and nanostructured multiphase polymer blend systems: phase morphology and interfaces. Boca Raton, FL, USA: CRC Press, Taylor and Francis Group; 2006. p. 391–420 [chapter 12].
[10] Arnal ML, Müller AJ, Maiti P, Hikosaka M. Nucleation and crystallization of isotactic poly(propylene) droplets in an immiscible polystyrene matrix. Macromol Chem Phys 2000;201(17):2493–504.
[11] Müller AJ, Balsamo V, Arnal ML. Nucleation and crystallization in diblock and triblock copolymers. Adv Polym Sci 2005;190:1–63.
[12] Turnbull D, Cormia RL. Kinetics of crystal nucleation in some alkane liquids. J Chem Phys 1961;34(3):820–31.
[13] Cormia RL, Price FP, Turnbull D. Kinetics of crystal nucleation in polyethylene. J Chem Phys 1962;37(6):1333–40.
[14] Koutsky JA, Walton AG, Baer E. Nucleation of polymer droplets. J Appl Phys 1967;38(4):1832–9.
[15] Turnbull D. Kinetics of solidification of supercooled liquid mercury droplets. J Chem Phys 1952;20(3):411–24.
[16] Kashchiev D, Kaneko N, Sato K. Kinetics of crystallization in polydisperse emulsions 1998;208:167–77.
[17] Perepezko JH, Höckel PG, Paik JS. Initial crystallization kinetics in undercooled droplets. Thermochim Acta 2001;388:129–41.
[18] Massa MV, Dalnoki-Veress K. Homogeneous crystallisation of poly(ethylene oxide) confined to droplets: the dependence of the crystal nucleation rate on length-scale and temperature. Phys Rev Lett 2004;92(25). Art. No. 255509.
[19] Barham PJ, Jarvis DA, Keller A. A new look at the crystallization of polyethylene. III. crystallization from the melt at high supercoolings. J Polym Sci Part B Polym Phys 1982;20(9):1733–48.
[20] Ibarretxe Uriguen J, Bremer L, Mathot VBF, Groeninckx G. Preparation of water-borne dispersions of polyolefins:new systems for the study of homogeneous nucleation of polymers. Polymer 2004;45:5961–8.
[21] Fillon B, Wittmann JC, Lotz B, Thierry A. Self-nucleation and recrystallization of isotactic polypropylene (α phase) investigated by differential scanning calorimetry. J Polym Sci Part B Polym Phys 1993;31:1383–93.
[22] Frensch H, Jungnickel BJ. Fractionated and self-seeded crystallization in incompatible polymer blends. Plast Rub Comp Proc Appl 1991;16(1):5–10.
[23] Arnal ML, Müller AJ. Fractionated crystallisation of polyethylene and ethylene/α-olefin copolymers dispersed in immiscible polystyrene matrices. Macromol Chem Phys 1999;200:2559–76.
[24] Tol RT, Minakov AA, Adamosky SA, Mathot VBF, Schick C. Metastability of polymer crystallites formed at low temperature studied by ultra fast

calorimetry: polyamide 6 confined in sub-micrometer droplets vs. bulk PA6. Polymer 2006;47(6):2172–8.
[25] De Rosa C, Guerra G, Napolitano R, Petraccone V, Pirozzi B. Conditions for the $\alpha 1$–$\alpha 2$ transition in isotactic polypropylene samples. Eur Polym J 1984;20(10):937–41.
[26] Brückner S, Meille SV, Petraccone V, Pirozzi B. Polymorphism in isotactic polypropylene. Prog Polym Sci 1991;16:1361–404.
[27] Müller AJ, Balsamo V, Arnal ML, Jakob T, Schmalz H, Abetz V. Homogeneous nucleation and fractionated crystallization in block copolymers. Macromolecules 2002;35:3048–58.
[28] Bartczak Z, Martuscelli E, Galeski A. Polypropylene: structure, blends and composites. In: Ch. primary spherulite nucleation in polypropylene-based blends and copolymers. Chapman and Hall; 1995. p. 25–49.
[29] Coupland JN. Crystallization in emulsions. Curr Opin Coll Int Sci 2002;7(5-6):445–50.
[30] Pyda M, editor. The ATHAS Data Bank, http://athas.prz.rzeszow.pl/.
[31] Calorimetry and thermal analysis of polymers. In: Mathot VBF, editor. Thermal characterization of states of matter. Munich, Vienna, New York: Hanser Publishers; 1994. p. 105–67 [chapter 5].
[32] Pound GM, LaMer VK. Kinetics of crystalline-nucleus formation in supercooled liquid tin. J Am Chem Soc 1952;74:2323–32.
[33] Jin Y, Hilter A, Baer E, Masirek R, Piorkowska E, Galeski A. Formation and transformation of smectic polypropylene nanodroplets. J Polym Sci Part B Polym Phys 2006;44(13):1795–803.
[34] Weber CH, Chiche A, Krausch G, Rosenfeldt S, Ballauff M, Harnau L, et al. Single lamella nanoparticles of polyethylene. Nano Lett 2007;7(7):2024–9.